4. Ternary electrodes under equilibrium or near-equilibrium (Huggins, ch. 4)

1. Ternary phase diagrams and phase stability diagrams
2. Influence of subtriangle configurations in ternary systems
3. An example: sodium/nickel chloride system
4. An example: lithium-copper-chloride system
5. Calculation of the maximum theoretical specific energies
6. An example: metal hydride systems
7. An example: lithium-transition metal oxides
8. Ternary systems composed of two binary metal alloys

1. Ternary Phase Diagrams and Phase Stability Diagrams

-isothermal Gibbs triangles

$$F = C - P + 2$$

If C =3, P = 3, F = 2. If the temperature and total pressure are kept constant, the number of residual degrees of freedom *F* will be zero

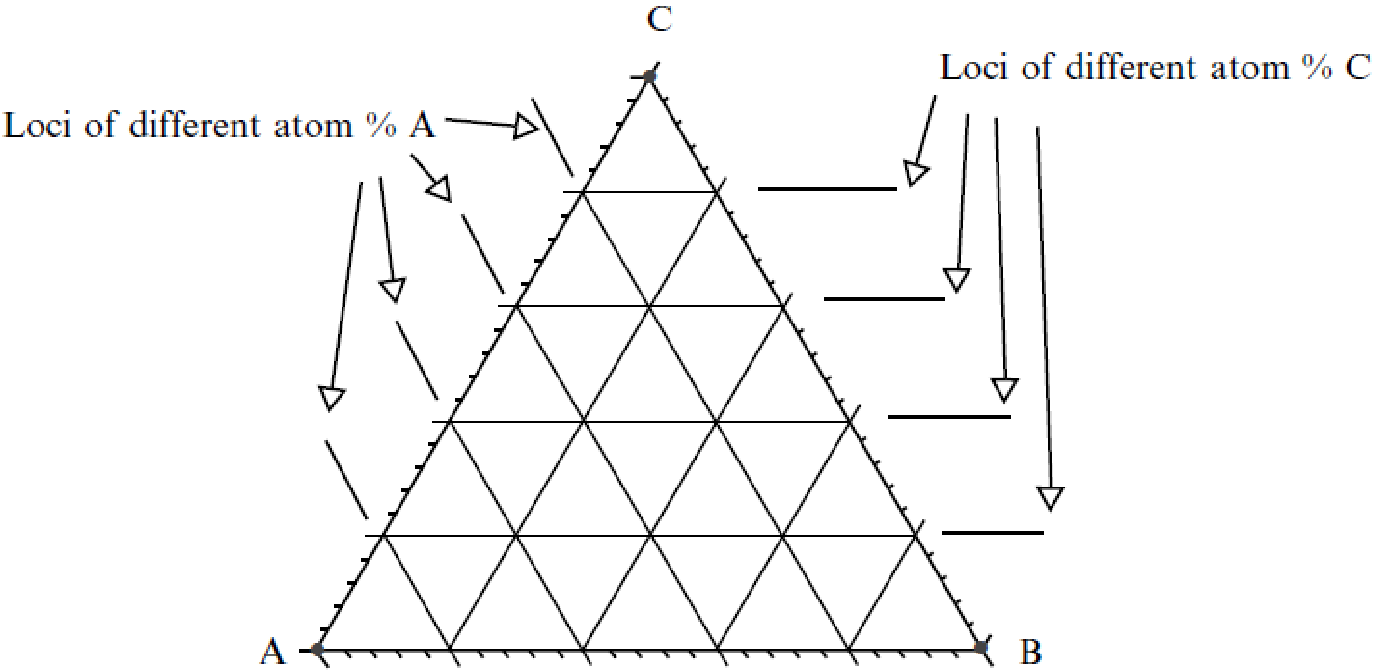

Fig. 4.1 General coordinate scheme used to depict compositions and phase equilibria in ternary systems on isothermal Gibbs triangles

-two-phase tie line : two phases are in equilibrium if their compositions are connected by a line → P = 2 on the line

-the Gibbs triangle is divided into *subtriangles* whose sides are *two-phase tie lines*

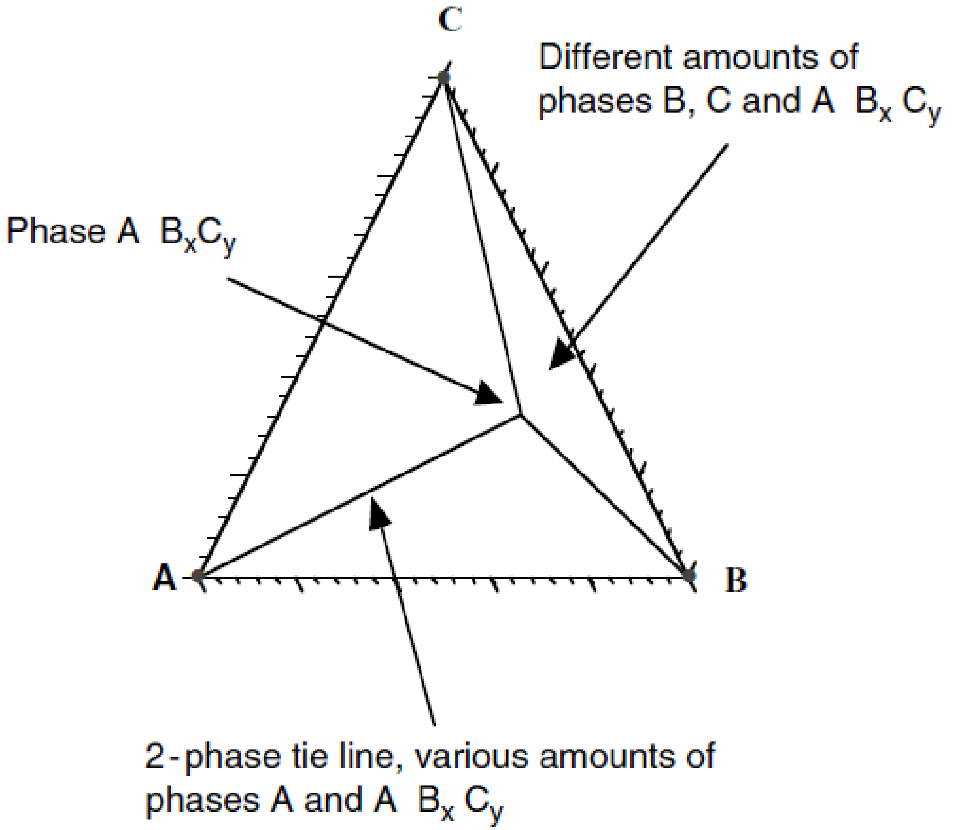

Fig. 4.2 Isothermal phase stability diagram ABC for the case in which there is a single intermediate phase whose composition is A_xB_yC

2. Comments on the Influence of SubTriangle Configurations in Ternary Systems

e.g. Li-M + X → Li–M–X
Assuming two stable binary phases, LiM, MX

If no X, Li-M edge → single Li-M system → M, LiM phases,
F = 2-2+2 = 2

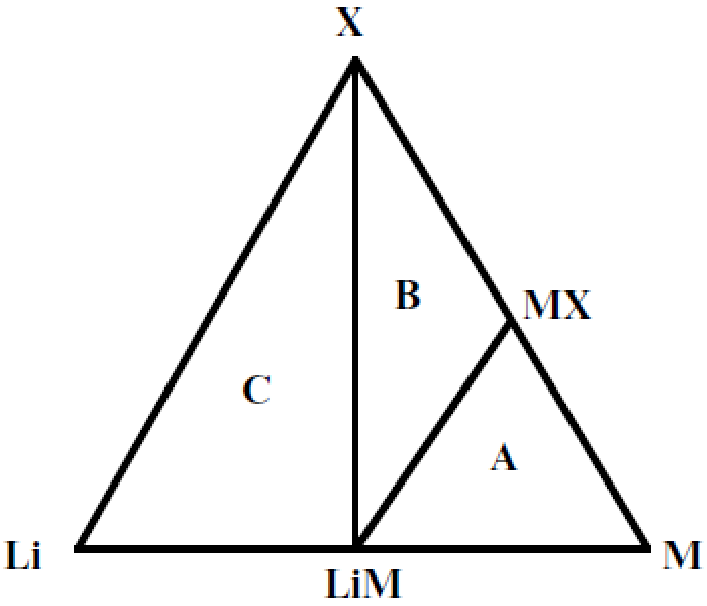

Fig. 4.3 Schematic ternary phase diagram for the Li–M–X system in which there are intermediate phases in the centers of both the Li–M and the M–X binary systems

-In triangle A

$$E_A = -\Delta G_f^\circ(\mathrm{LiM})/F$$

-Now if X added?

→ starting from X-M side, goes in the direction of Li corner (dotted lines).

-In A, F = 3–3+2 = 2, plateau, however, its length will vary depending upon the starting composition

-Li↑ → enter into triangle B → additional plateau,

F = 3–3+2 = 2

potential $E_B = -(\Delta G_f^\circ(\mathrm{MX}) - \Delta G_f^\circ(\mathrm{LiM}))/F$

-Further Li↑ → enter triangle C → potential will be the same as that of pure lithium

Fig. 4.4, Fig 4.5

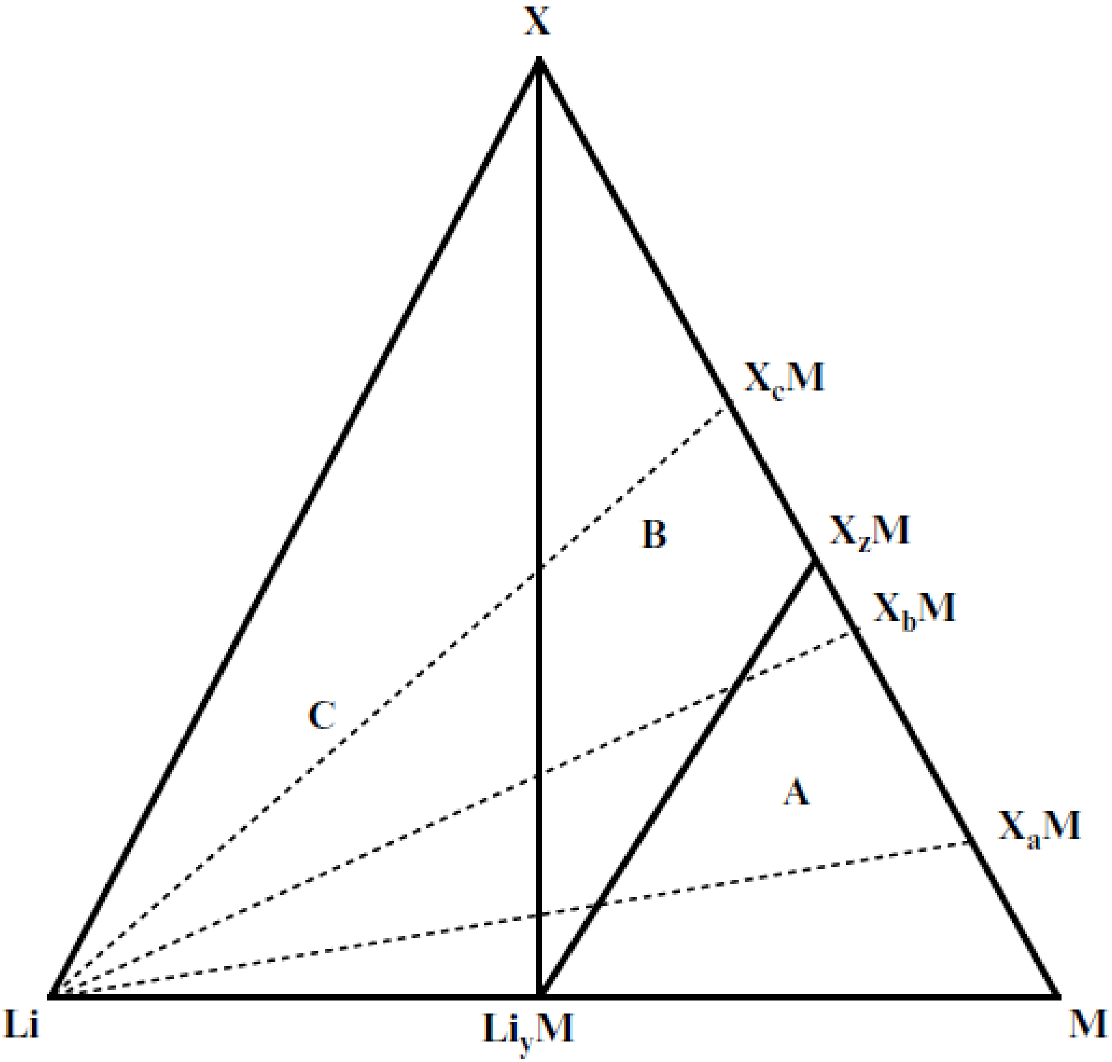

Fig. 4.4 The ternary Li–M–X system shown in Fig. 4.3, displaying the loci of the overall composition for three different initial compositions

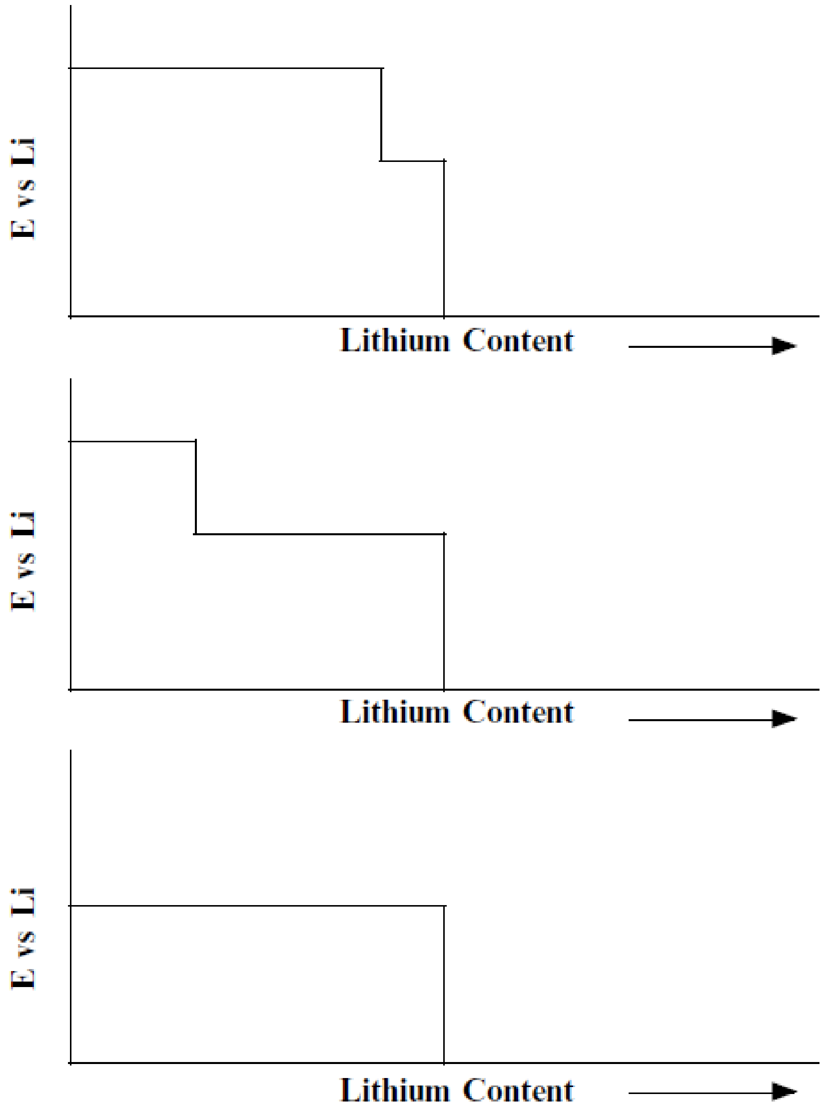

Fig. 4.5 Variation of the potential as lithium is added to electrodes with the three different starting compositions shown in Fig. 4.4. *Top* X_aM, *middle* X_bM, and *bottom* X_cM

-another case: additional Li-X binary system (intermediate phase)

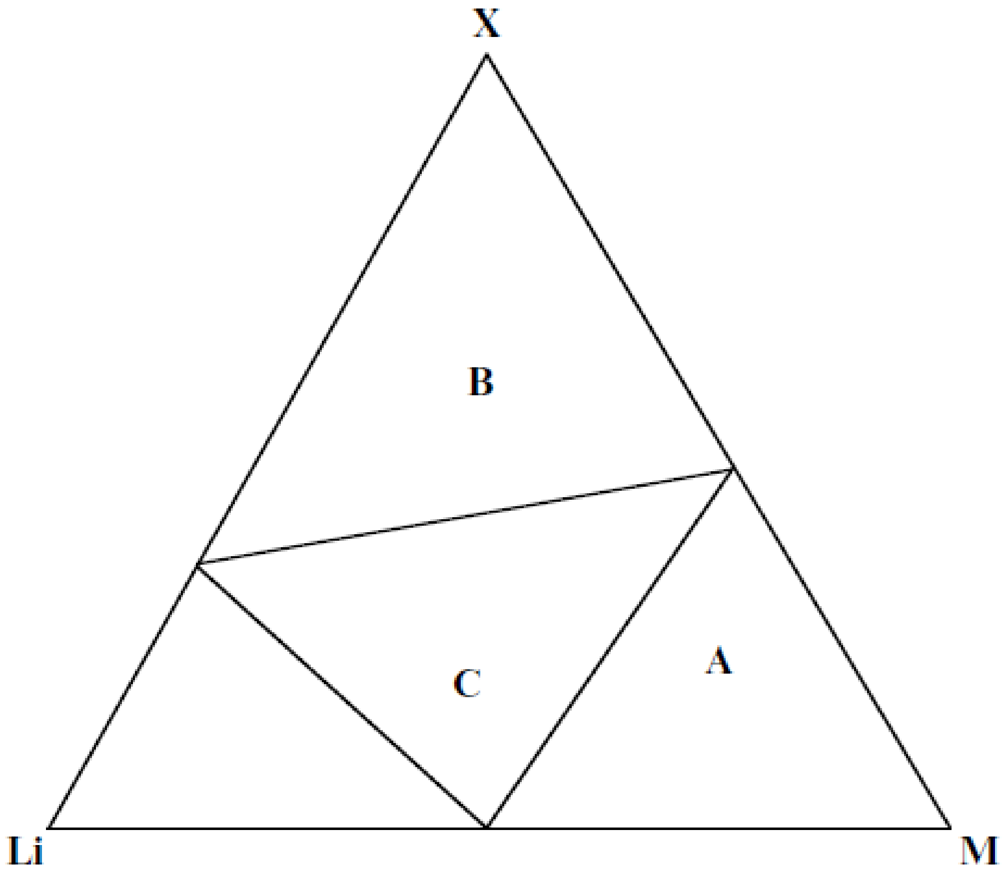

Fig. 4.6 Hypothetic ternary phase diagram in which there is one intermediate phase in each of the binary systems

3. An Example: Sodium/Nickel Chloride “Zebra” System

-solid electrolyte: sodium beta alumina

-operates at 250–300 °C

-liquid sodium as the negative electrode, which is enclosed in a solid β-aluminum tube

-positive electrode: finely powdered $NiCl_2$ inside a 2nd (liquid) electrolyte, $NaAlCl_4$

Na/Naβ-alumina/$NaAlCl_4$, $NiCl_2$

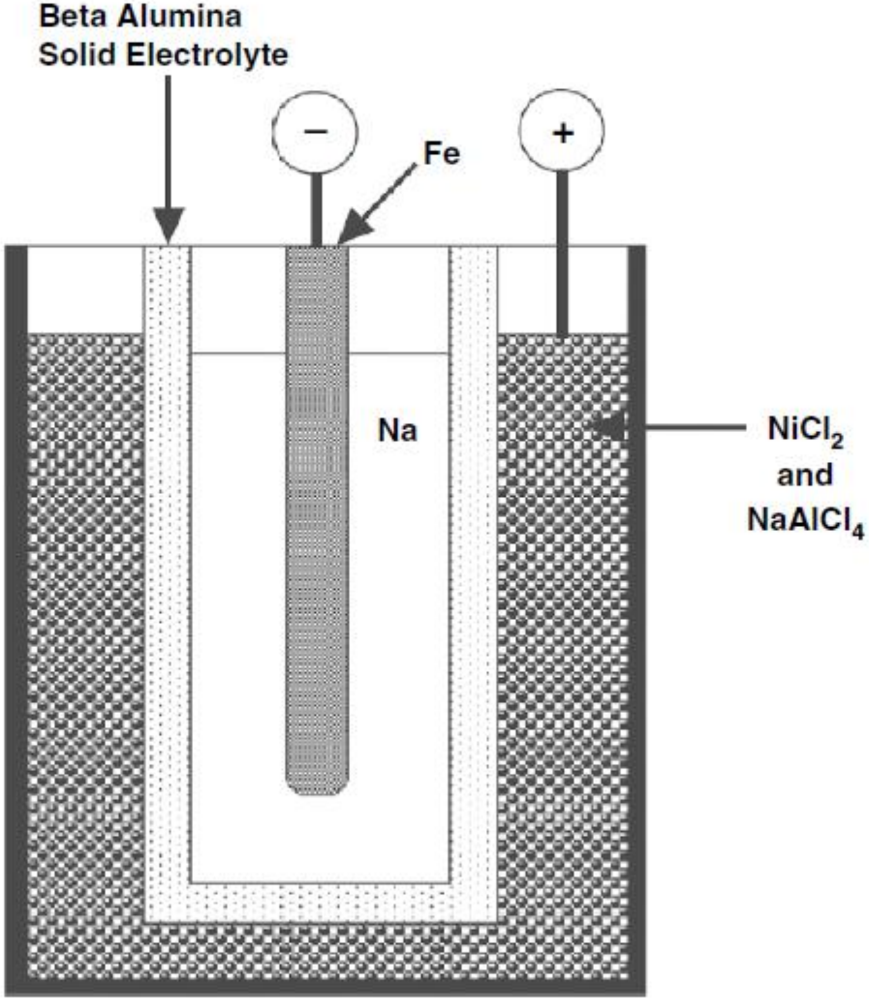

Fig. 4.7 Schematic view of the “Zebra” cell, which operates at 250–300°C

- Na–Ni–Cl ternary phase diagram

Thermodynamic data indicate that there are only two binary phases in this ternary system, $NiCl_2$ and NaCl → two possibilities: either a tie line from $NiCl_2$ to the Na corner, or there is one from NaCl to the Ni corner

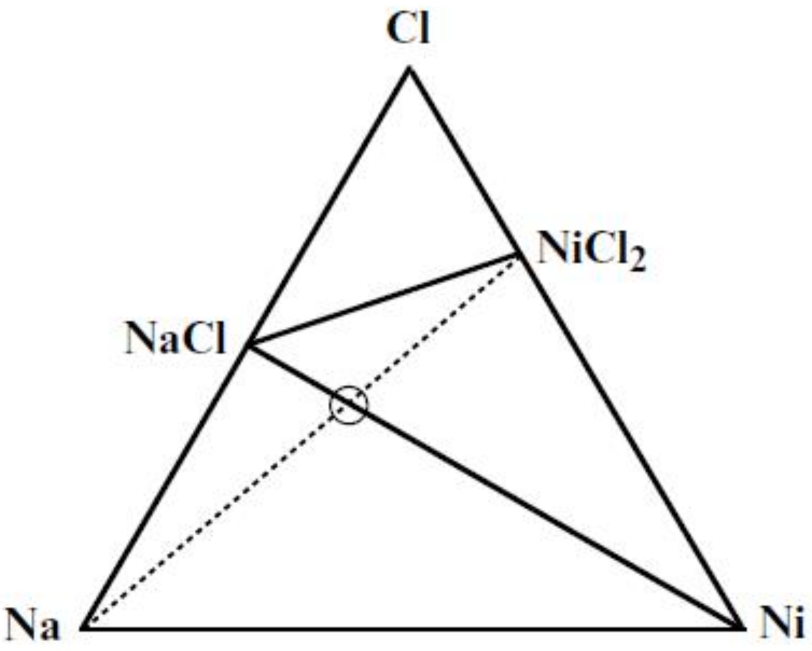

Fig. 4.8 The Na–Ni–Cl ternary phase diagram, showing the locus of the overall composition as Na reacts with $NiCl_2$

$$2Na + NiCl_2 = 2NaCl + Ni$$

The Gibbs free energy change in this virtual reaction

$$\Delta G_r^\circ = 2\Delta G_f^\circ(NaCl) - \Delta G_f^\circ(NiCl_2)$$

standard Gibbs free energies at 275℃ of NaCl and $NiCl_2$ are −360.25 and −221.12 kJ/mol → reaction tends to go to the right and the tie line between NaCl and Ni is more stable than the one between $NiCl_2$ and Na (solid line)

-As Na reacts with $NiCl_2$ the overall composition of the positive electrode follows the dotted line. When it reaches the composition indicated by the small circle, all the $NiCl_2$ will have been consumed, and only NaCl and Ni are present

-in the NaCl–$NiCl_2$–Ni triangle, the potential is constant. Its value can be calculated from the Gibbs free energy of reaction value. The voltage of the positive electrode with respect to the pure Na negative electrode

$$\Delta E = -\Delta G_r/zF$$

where z = 2 → 2.59 V in Zebra cell

HW#7

4. Second Example: Lithium–Copper–Chlorine Ternary System

-Thermodynamic information shows that there are three stable phases within this system at 298 K, LiCl, CuCl, and $CuCl_2$. Values of their standard Gibbs free energies of formation are given in Table 4.1 → to determine the stable tie lines

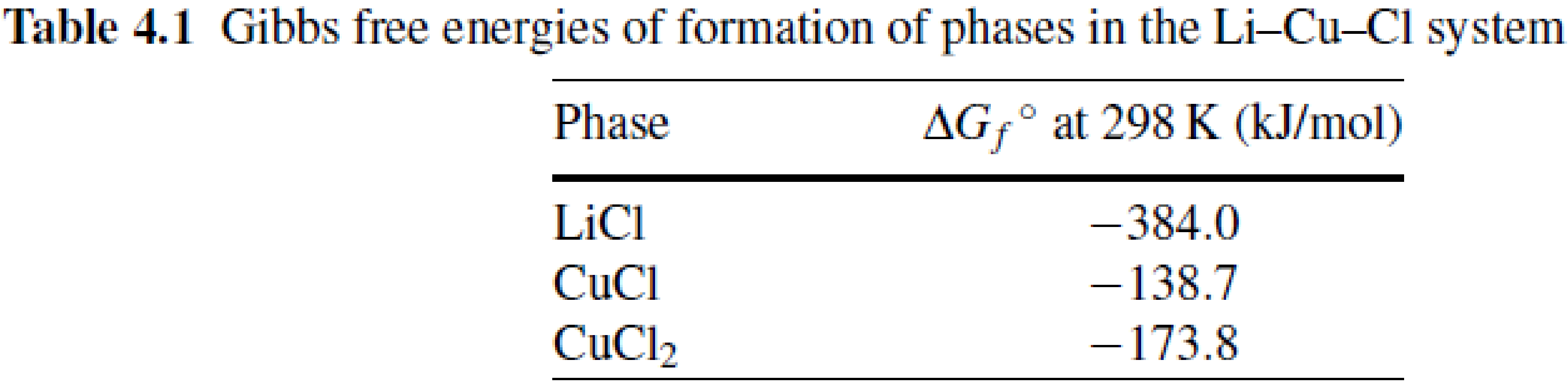

Table 4.1 Gibbs free energies of formation of phases in the Li–Cu–Cl system

Phase	$\Delta G_f{}^\circ$ at 298 K (kJ/mol)
LiCl	-384.0
CuCl	-138.7
$CuCl_2$	-173.8

- A few simple rules and procedures

(1) The total area must be divided into triangles. Their edges are tie lines between pairs of phases.

(2) No more than three phases can be present within a triangle. Their compositions must be at the corners.

(3) Tie lines cannot cross.

-The line between LiCl and $CuCl_2$ must be stable, as there are no other possible lines that could cross it. There are four additional possibilities, lines between Li and $CuCl_2$, Li and CuCl, LiCl and CuCl, and LiCl and Cu → virtual reactions to determine thermodynamically which one is stable

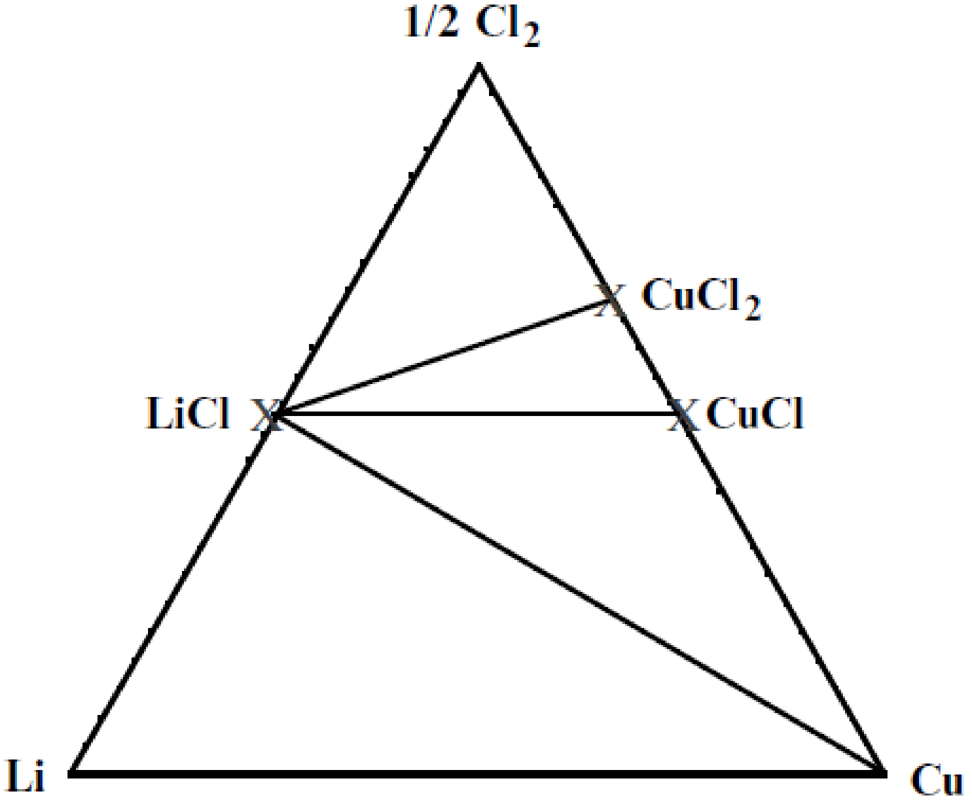

Fig. 4.9 Isothermal phase stability diagram for the Li–Cu–Cl ternary system at 25°C

e.g. tie line between LiCl and Cu or one between CuCl and Li? Both cannot be stable, for they would cross.

→ The virtual reaction between the pairs

$$\mathrm{LiCl+Cu = CuCl+Li}$$

the standard Gibbs free energy of reaction

$$\Delta G_r^\circ = \Delta G_f^\circ(\mathrm{CuCl}) - \Delta G_f^\circ(\mathrm{LiCl})$$

→ ΔGr° is (−138.7)−(−384.0)=+245.3kJ/mol → this reaction would tend to go to the left → the combination of the phases LiCl and Cu is more stable than the combination of CuCl and Li → tie line between LiCl and Cu is stable in the phase diagram

-tie line between LiCl and Cu or one between $CuCl_2$ and Li?

$$\mathrm{2LiCl+Cu = CuCl_2 + 2Li}$$

the standard Gibbs free energy of reaction

$$(-173.8)-2(-384.0) = +594.2\text{kJ/mol.}$$

→ The resulting isothermal phase stability diagram for this system is shown in Fig. 4.9

4.1. Calculation of the Voltages in This System

(i) Reaction with Li with CuCl : Li↑ → dotted line → it moves into and across LiCl-CuCl-Cu triangle. Inside this triangle, F = 3–3+2 = 2 , potential plateau

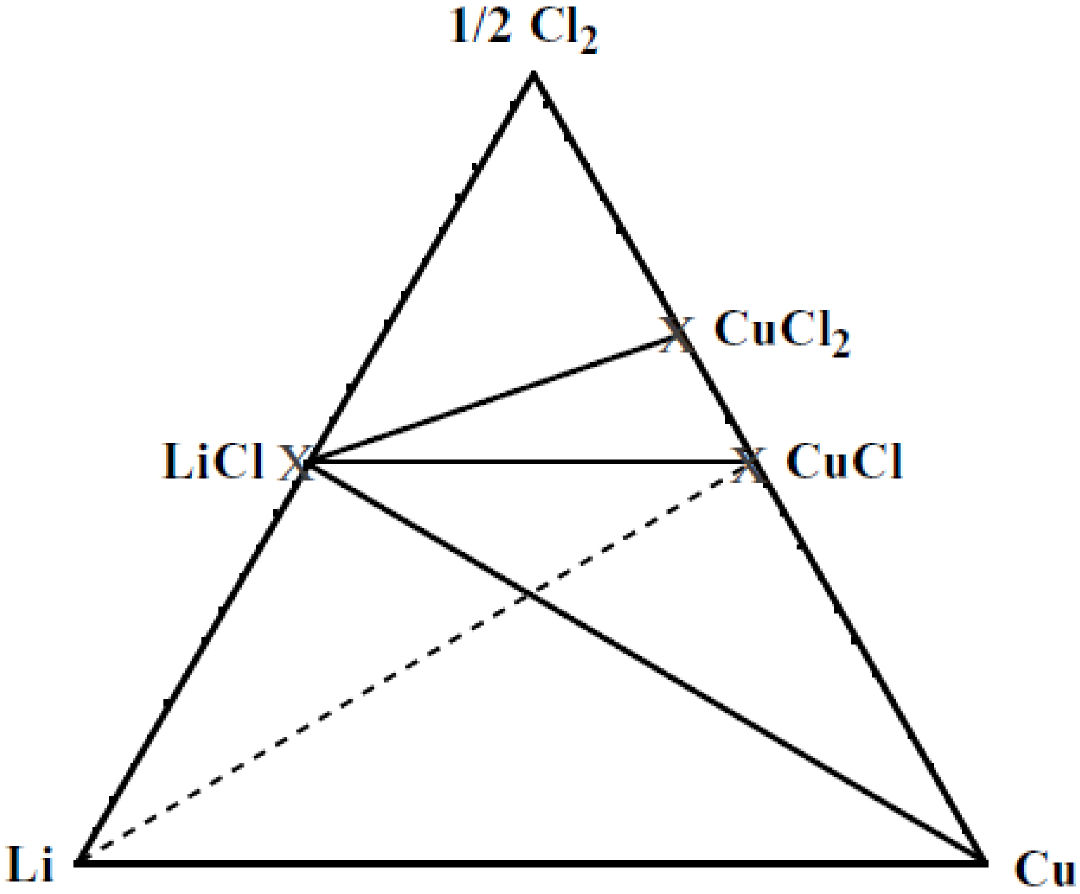

Fig. 4.10 Use of ternary phase diagram to understand the reaction of lithium with CuCl

-phase diagram → up to 1 mol of Li can participate in this rxn

$$Li + CuCl = LiCl + Cu$$

standard Gibbs free energy: (−384.0)-(−138.7) = -245.3kJ/mol

→ E = 2.54 V vs. pure Li

HW#7

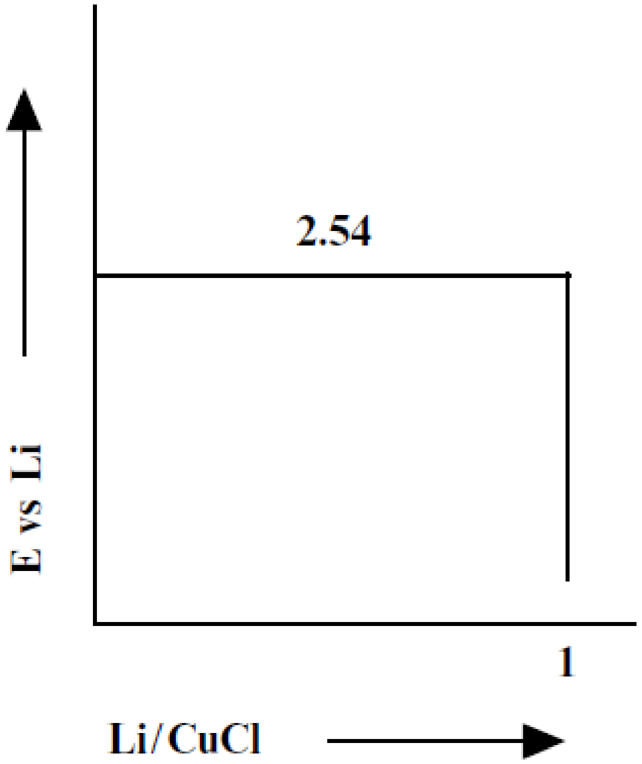

Fig. 4.11 Variation of the equilibrium voltage of Li/CuCl cell as a function of the extent of reaction

(ii) If the positive electrode $CuCl_2$ instead of CuCl

1st, LiCl-$CuCl_2$-CuCl triangle → $F = 3–3+2 = 2$ (plateau)

$$Li+CuCl_2 = LiCl+CuCl$$

The standard Gibbs free energy change:

$(−384.0)+(−138.7)−(−173.8) = −348.9$ kJ/mol

→ $E = 3.615$ V vs. pure Li

HW#7

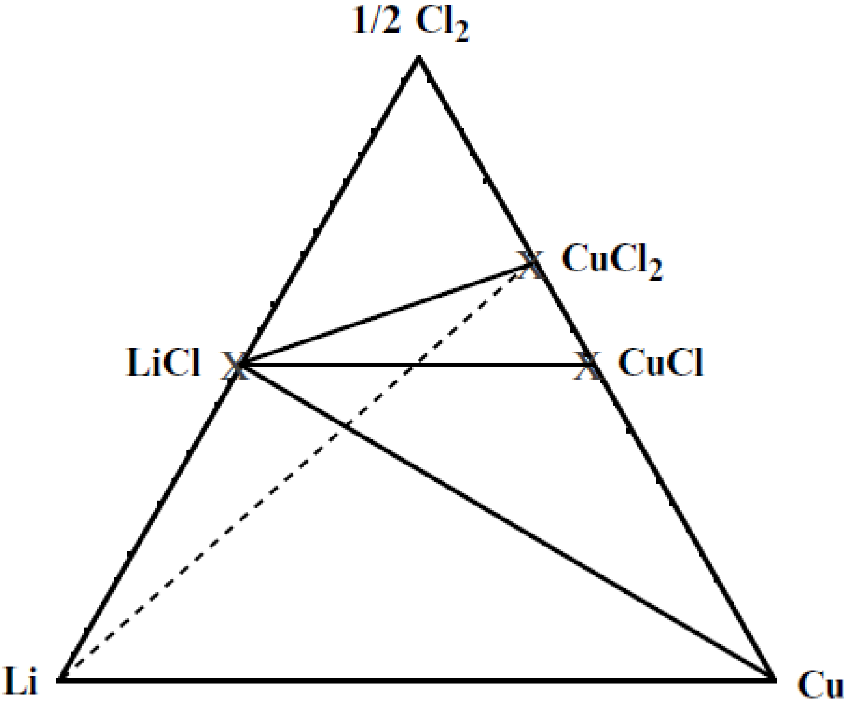

Fig. 4.12 Use of ternary phase stability diagram to understand the reaction of Li with $CuCl_2$

-further Li↑ → 2^{nd} triangle LiCl-CuCl-Cu → 2.54 V

→ two plateaus

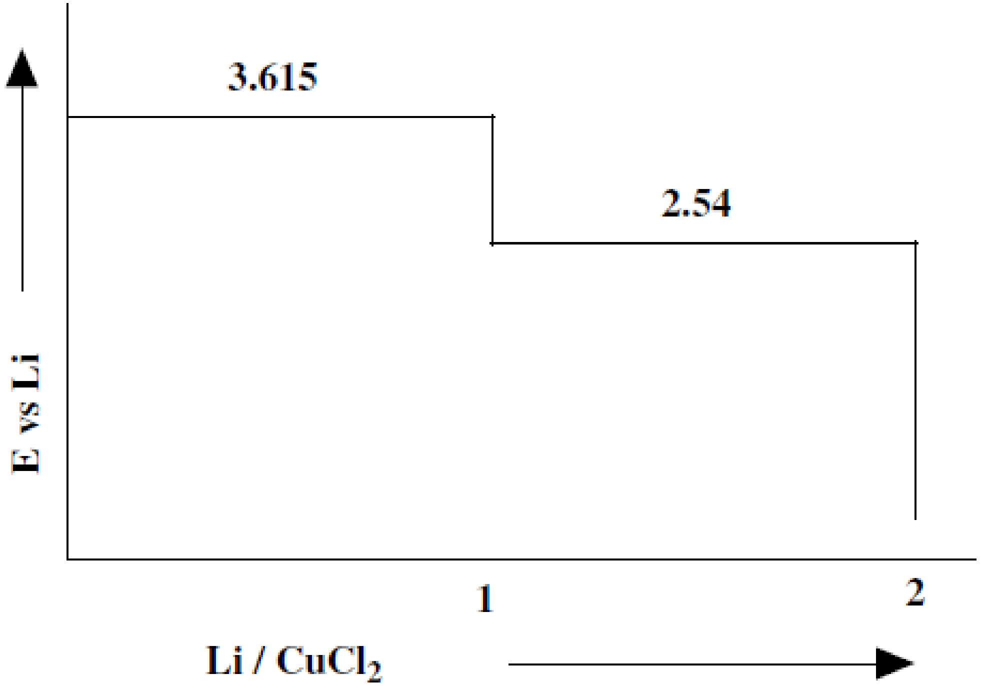

Fig. 4.13 Equilibrium titration curve for the reaction of lithium with $CuCl_2$ to form LiCl and CuCl, and then more LiCl and Cu

5. Calculation of the Maximum Theoretical Specific Energies of Li/CuCl and Li/$CuCl_2$ Cells

-the maximum theoretical specific energy (MTSE)

$$MTSE = (xV/W)(F)\ kJ/kg$$

where x is the number of moles of Li involved in the reaction, V the average voltage, and W the sum of the atomic weights of the reactants. F is the Faraday constant, 96,500 coulombs per mole

-MTSE for CuCl (react with Li):
W = (7+63.55+35.45) = 106.0g, x = 1, V = 2.54V → MTSE = 2,312.4 kJ/kg = 642.3 Wh/kg

-MTSE for $CuCl_2$ to form LiCl + CuCl :
W = 141.45g, x = 1, V = 3.615 V → MTSE = 2466.2 kJ/kg = 685.1 Wh/kg

HW#7

-If further lithium reacts with the products of this reaction, the voltage will proceed along the lower plateau, as was the case for an electrode whose composition started as CuCl. Thus additional energy is available. However, the total specific energy is not simply the sum of the specific energies that have just been calculated for the two plateau reactions independently. The reason for this is that the weight that must be considered in the calculation for the second reaction is the starting weight before the first reaction in this case.

for 2nd plateau reaction:
MTSE = (1)(2.54)(96,500)/141.45 = 1,732.8kJ/kg
This is less than for the second plateau alone, starting with CuCl, which was shown earlier to be 2,312 kJ/kg. Alternatively, the specific energy content of the second plateau for an electrode that starts as $CuCl_2$ is 481.3Wh/kg instead of 642.3Wh/kg, if it were to start as CuCl.
Thus if the electrode starts out as $CuCl_2$, the total MTSE can be written as
MTSE = 2,466.2+1,732.8 = 4,199kJ/kg
Or alternatively, 685.1+481.3 = 1,166.4Wh/kg

6. An example: metal hydride systems

-Binary alloys are often used as negative electrodes in hydrogen-transporting electrochemical cells. When they absorb or react with hydrogen, they are generally called *metal hydrides*. Because of the presence of hydrogen as well as the two metal components, they become ternary systems

-hydrogen storage: great interest

$$E = (RT/zF)\Delta \ln p(H_2)$$

where $\Delta \ln p(H_2)$ is the difference in the natural logarithms of the effective partial pressures, or activities, of hydrogen at the two electrodes

-specific capacity: hydrogen storage per unit weight of host material

-Mg, 24.3g/mol. MgH_2 contains one mole of H_2, and the ratio 2/24.3 means 8.23 w/% hydrogen. This can be readily converted to the amount of charge stored
per unit weight, i.e., the number of mAh/g. One Faraday is 96,500 coulombs, or 26,800 mA h, per equivalent. The addition of two hydrogens per magnesium means
that two equivalents are involved. Thus 2,204 mA h of hydrogen can be reacted per gram of magnesium.

-On the other hand, one is often interested in the amount of hydrogen that can be obtained by the decomposition of a metal hydride. This means that the weight to be considered is that of the metal plus the hydrogen, rather than just the metal itself. When this is done, it is found that 7.6 w/%, or 2,038mA h/g hydrogen can be obtained from MgH_2.

-These values for magnesium are over five times those of the materials that are commonly used as metal hydride electrodes in commercial battery systems.

-Practical problem of magnesium: forms a very stable oxide, which acts as a barrier to the passage of hydrogen. It is very difficult to prevent the formation of this oxide on the alloy surface in contact with the aqueous electrolytes commonly used in battery systems containing metal hydrides
→ one strategy: put a material such as nickel, which is stable in these electrolytes, on the surface of the magnesium. It is known that nickel acts as a mixed conductor, allowing the passage of hydrogen into the interior of the alloy. However, this surface covering cannot be maintained over many charge/discharge cycles, with the accompanying volume changes
→ a different approach: use an electrolyte in which magnesium is stable, but its oxide is not. e.g.,
alkali organo-aluminate molten salt electrolyte $NaAlEt_4$

-Mg-Ni binary phase diagram: two phases Mg_2Ni, $MgNi_2$

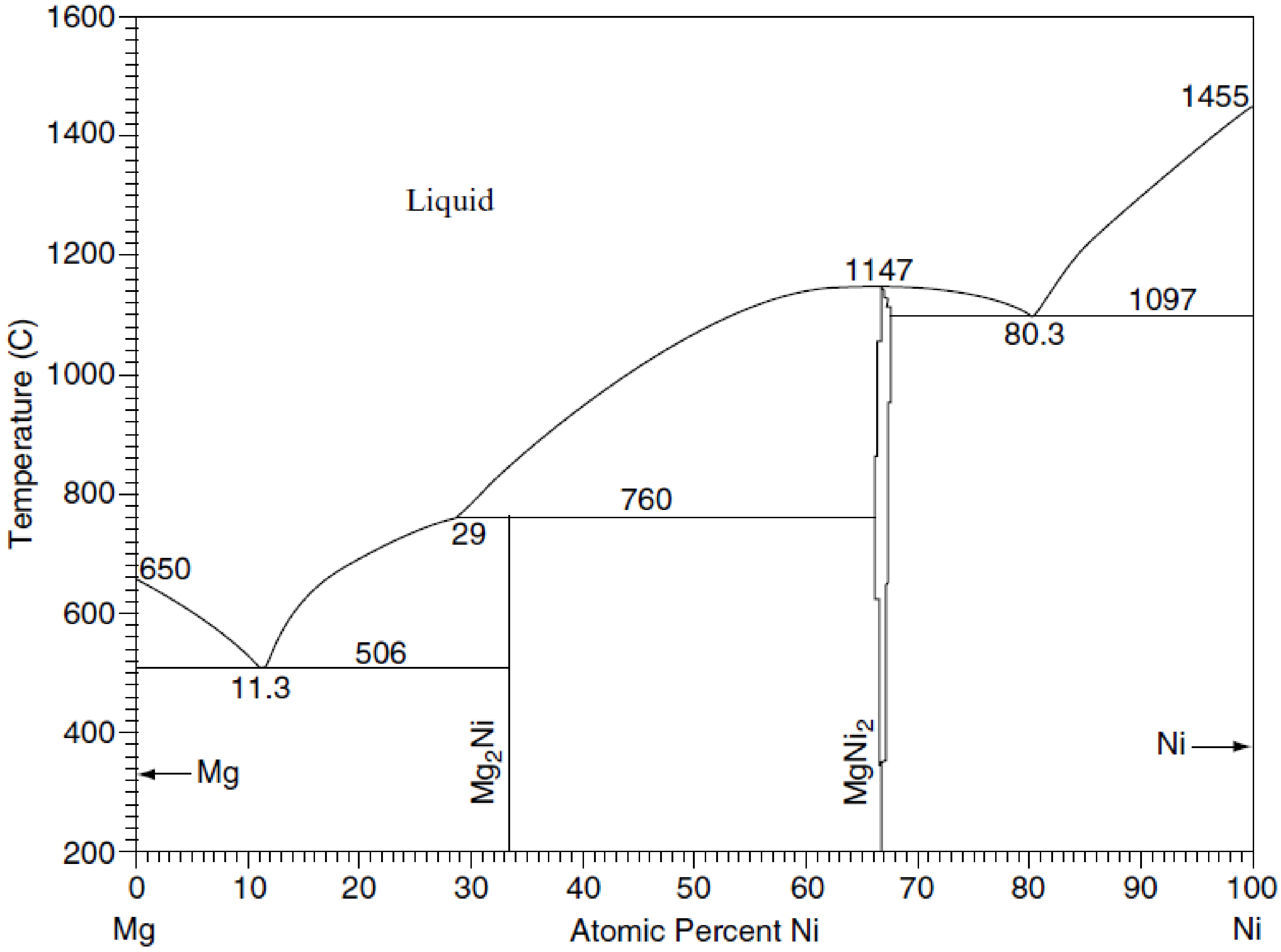

Fig. 4.14 Magnesium–nickel binary phase diagram

- Hydrogen →H-Mg-Ni ternary phase diagram: MgH_2

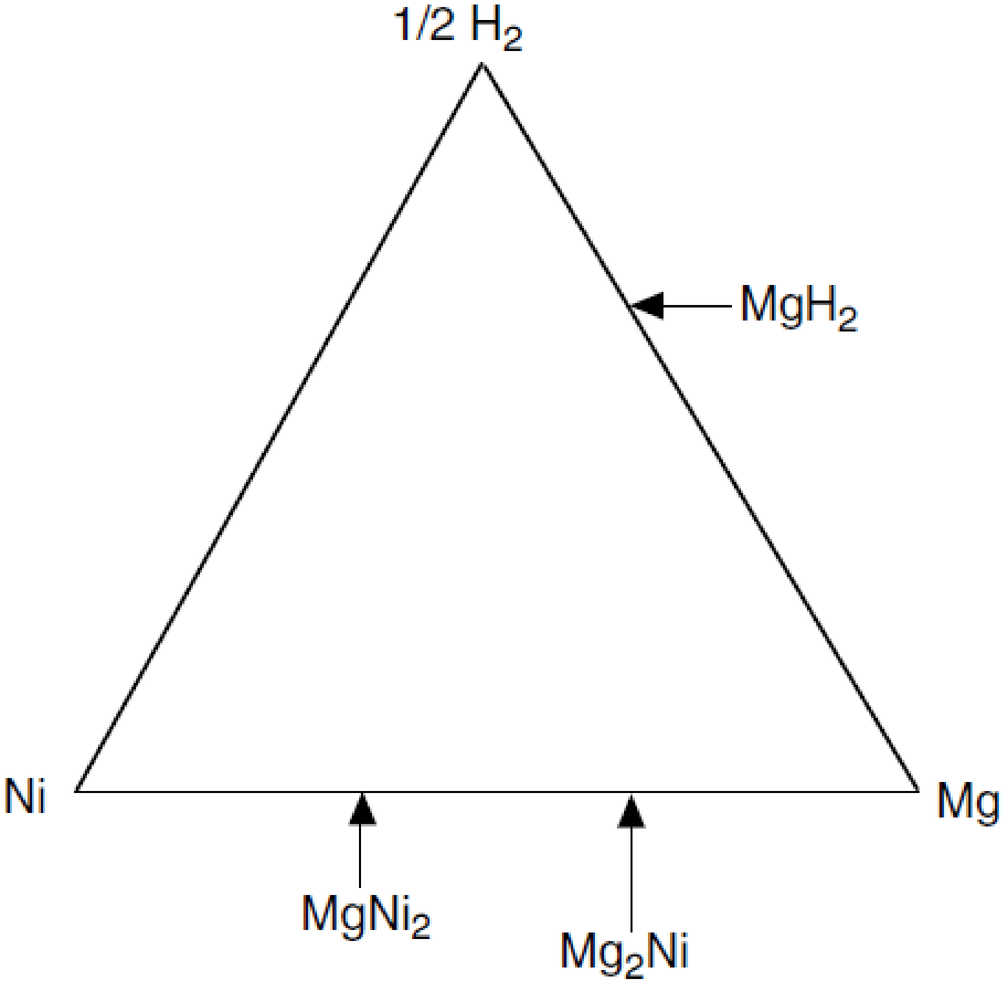

Fig. 4.15 The H–Mg–Ni ternary diagram showing only the known compositions along the binary edges

-an electrochemical cell: reaction of hydrogen with three compositions in this binary alloy system, $MgNi_2$, Mg_2Ni, and $Mg_{2.35}Ni$ → dashed lines shown as hydrogen was added

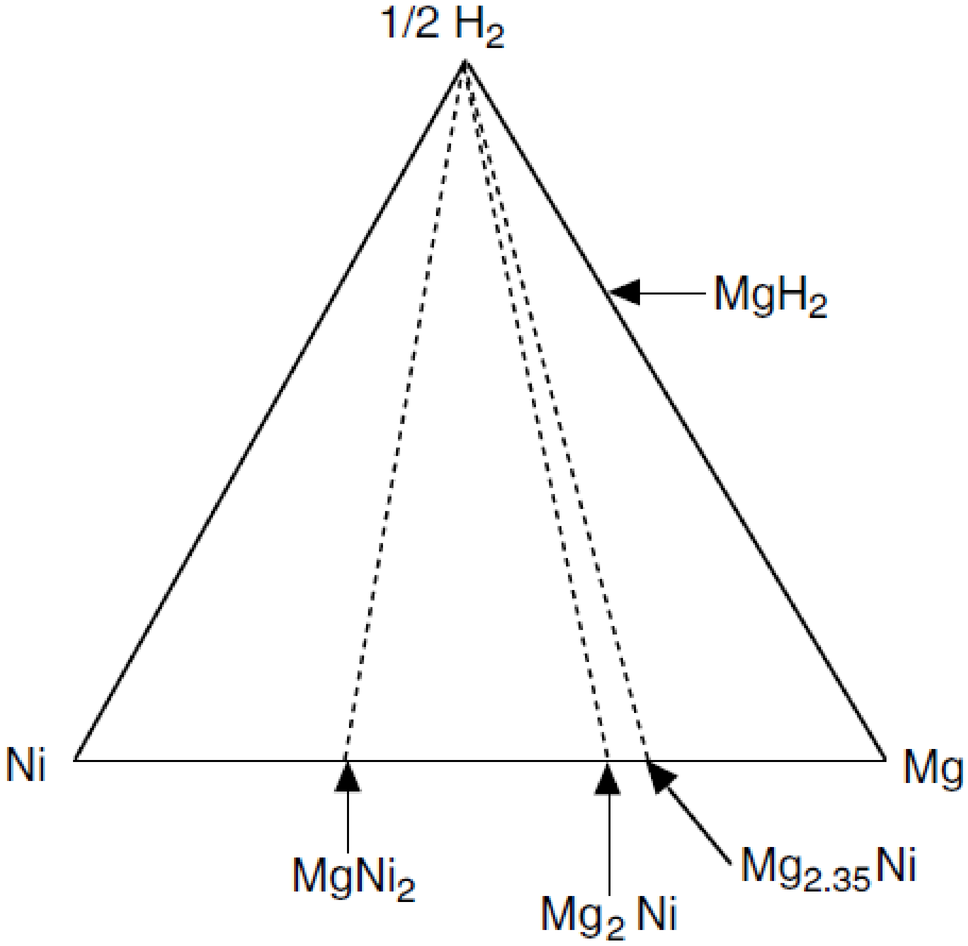

Fig. 4.16 Loci of the overall composition as hydrogen reacts with three initial Mg–Ni alloy compositions

-It was found that the voltage went to zero as soon as hydrogen was added to the phase $MgNi_2$. However, in the other cases, it changed suddenly from one plateau potential to another as certain compositions were reached. These transition

compositions are indicated by the circles in Fig. 4.17. The values of the voltage vs. the hydrogen potential in the different compositions regions are also shown in that figure → constant potential plateaus are found for compositions in three-phase triangles, and potential jumps occur when the composition crosses two-phase tie lines

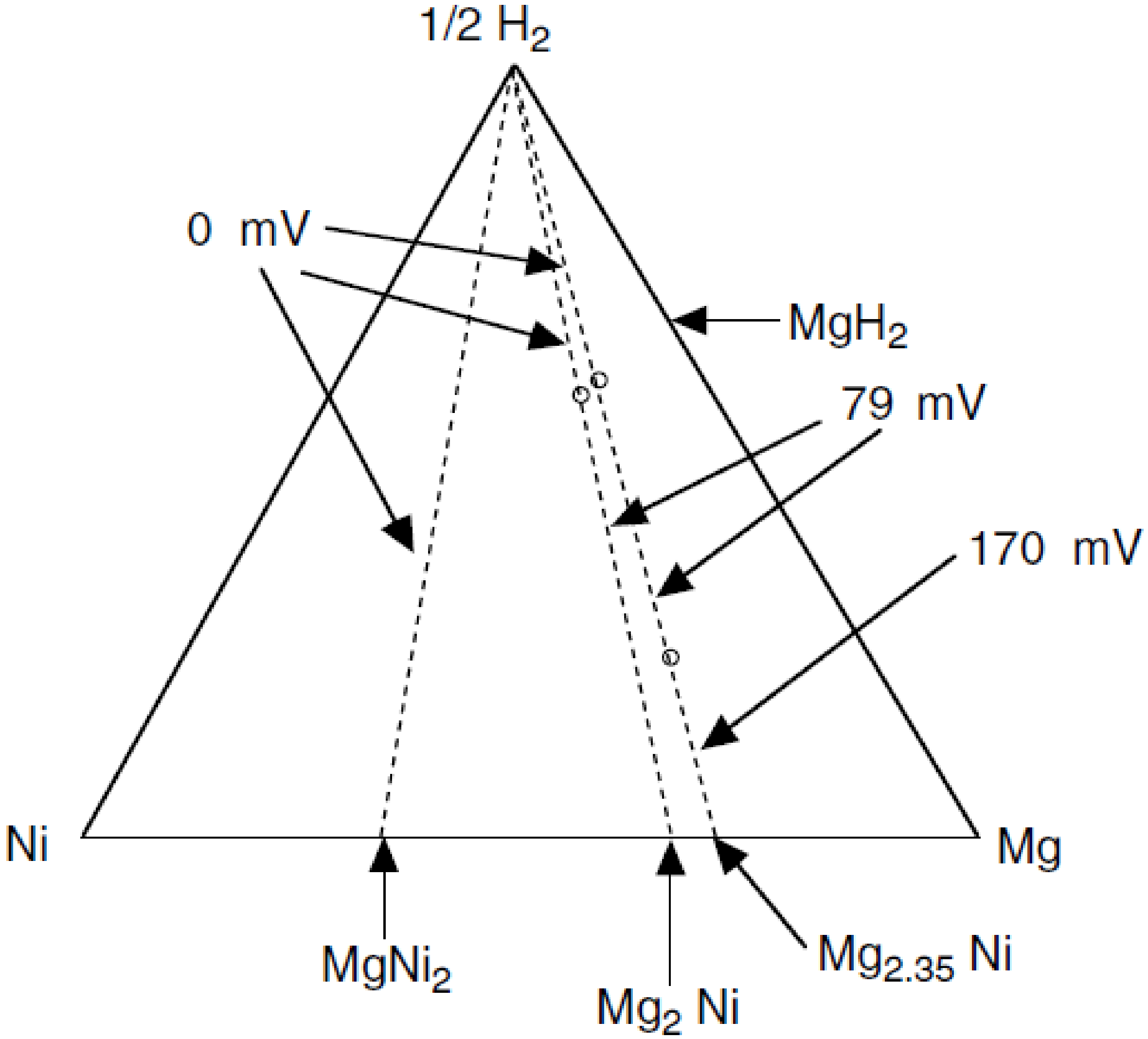

Fig. 4.17 Plateau voltages found in different composition regions

-no phases between $MgNi_2$ and pure hydrogen, but there must be a ternary phase with the composition Mg_2NiH_4

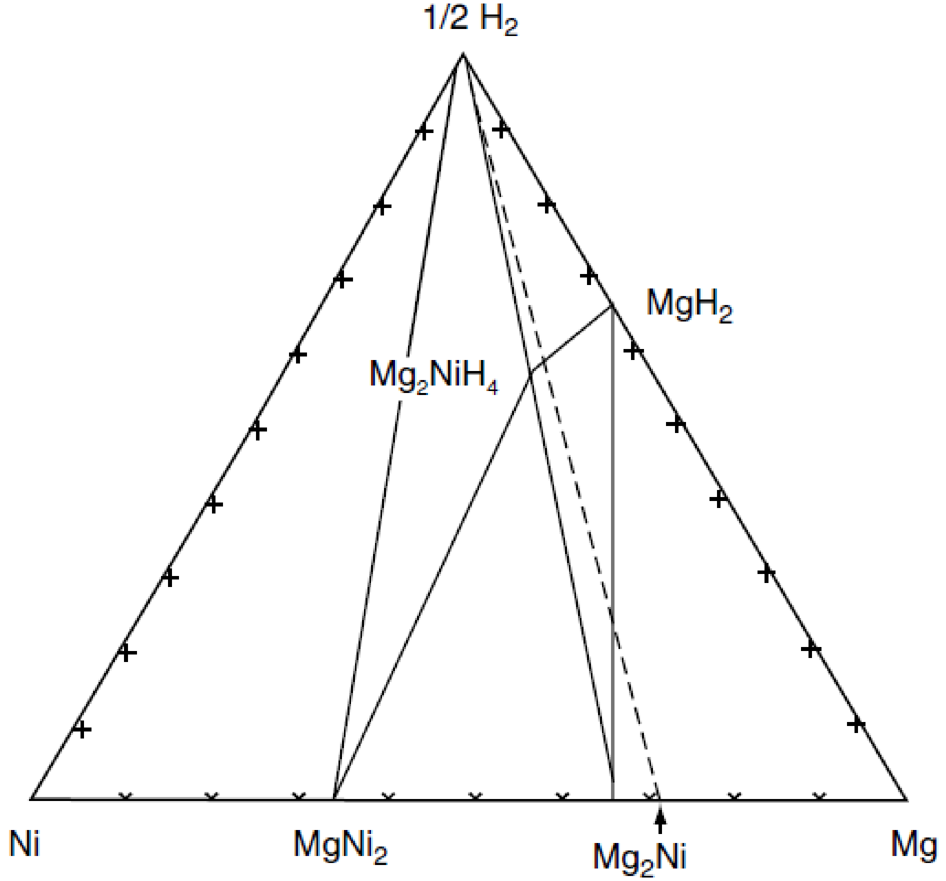

Fig. 4.18 Ternary phase stability diagram for the H–Mg–Ni system at about 140°C, derived from the compositional variation of the potential as hydrogen was reacted with three different initial binary alloy compositions

-The phase Mg_2Ni reacts with four hydrogen atoms to form Mg_2NiH_4 at a constant potential of 79mV vs. pure hydrogen. The weight of the Mg_2Ni host is 107.33g, which is 26.83 g/mol of hydrogen atoms. This amounts to 3.73% hydrogen atoms stored per unit weight of the initial alloy. This is quite attractive and is considerably more than the specific capacity of the materials that are currently used in the negative electrodes of metal hydride/H_xNiO_2 batteries

- Pure magnesium reacts to form MgH_2 at a constant potential of 107mV vs. pure hydrogen→ this amounts to 8.23% hydrogen atoms per unit weight of the initial magnesium, or 7.6w% relative to MgH_2

$Mg_{2.35}Ni$: two potential plateaus, and their respective lengths, as well as the total amount of hydrogen stored per unit weight of the electrode, will have intermediate values, varying with the initial composition. As an example, the variation of the potential with the amount of hydrogen added to the $Mg_{2.35}Ni$ is shown in Fig. 4.19

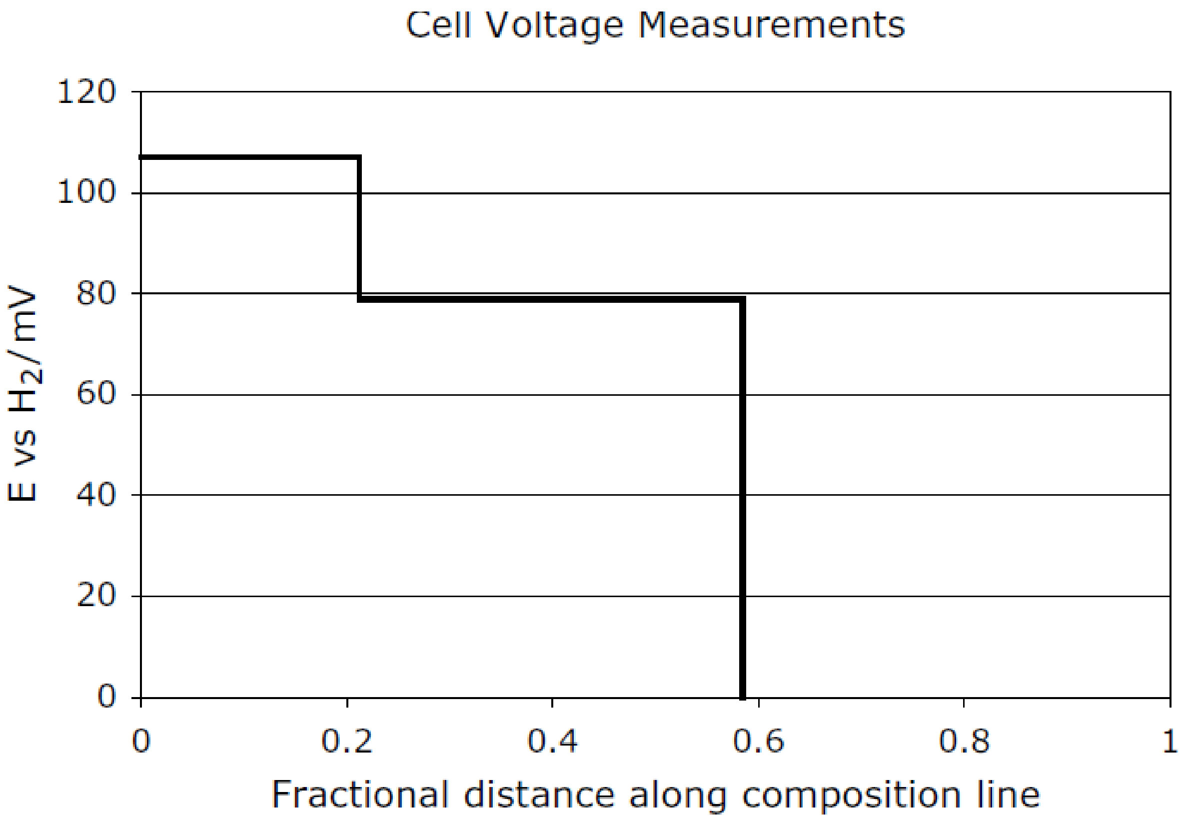

Fig. 4.19 Variation of potential as hydrogen is added to alloy with initial composition $Mg_{2.35}Ni$

H-Mg-Cu

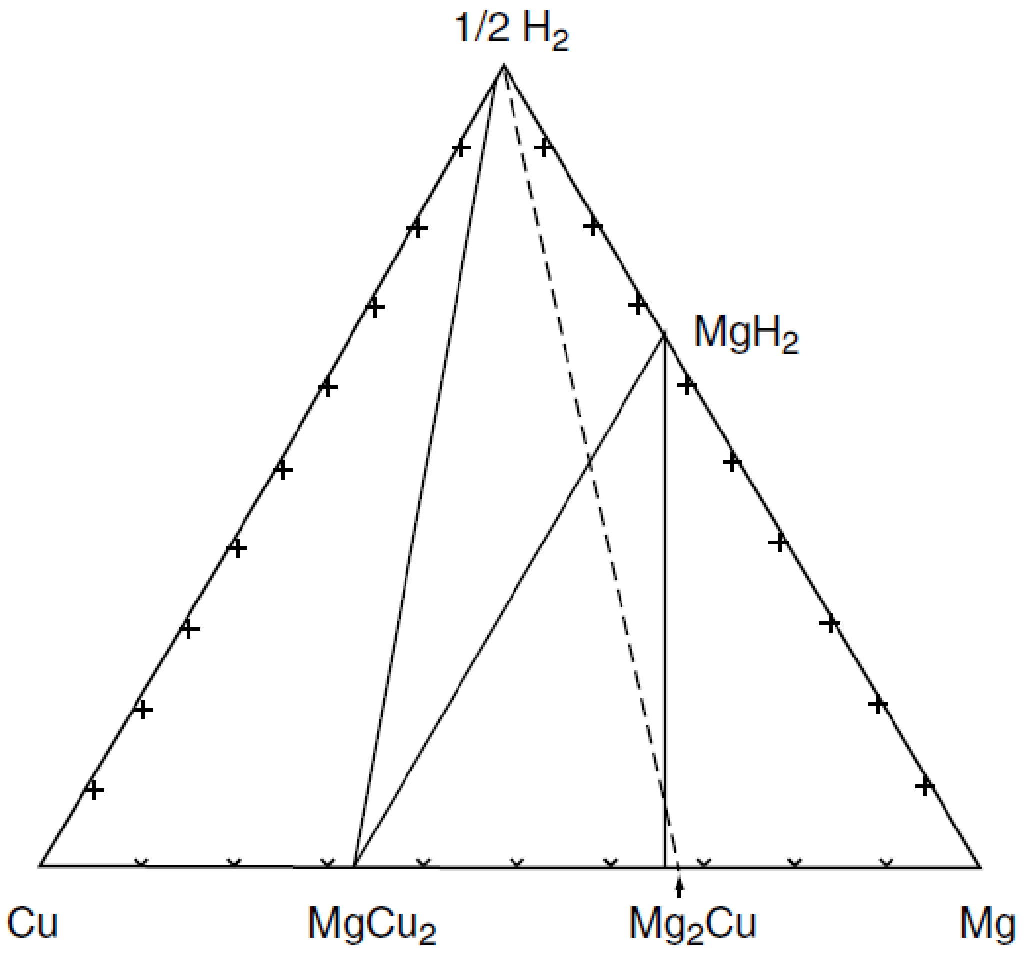

Fig. 4.20 Ternary phase stability diagram for the H–Mg–Cu system at about 140°C, derived from the compositional variation of the potential as hydrogen was reacted with different initial binary alloy compositions using organic anion molten salt electrolyte

H-Mg-Al

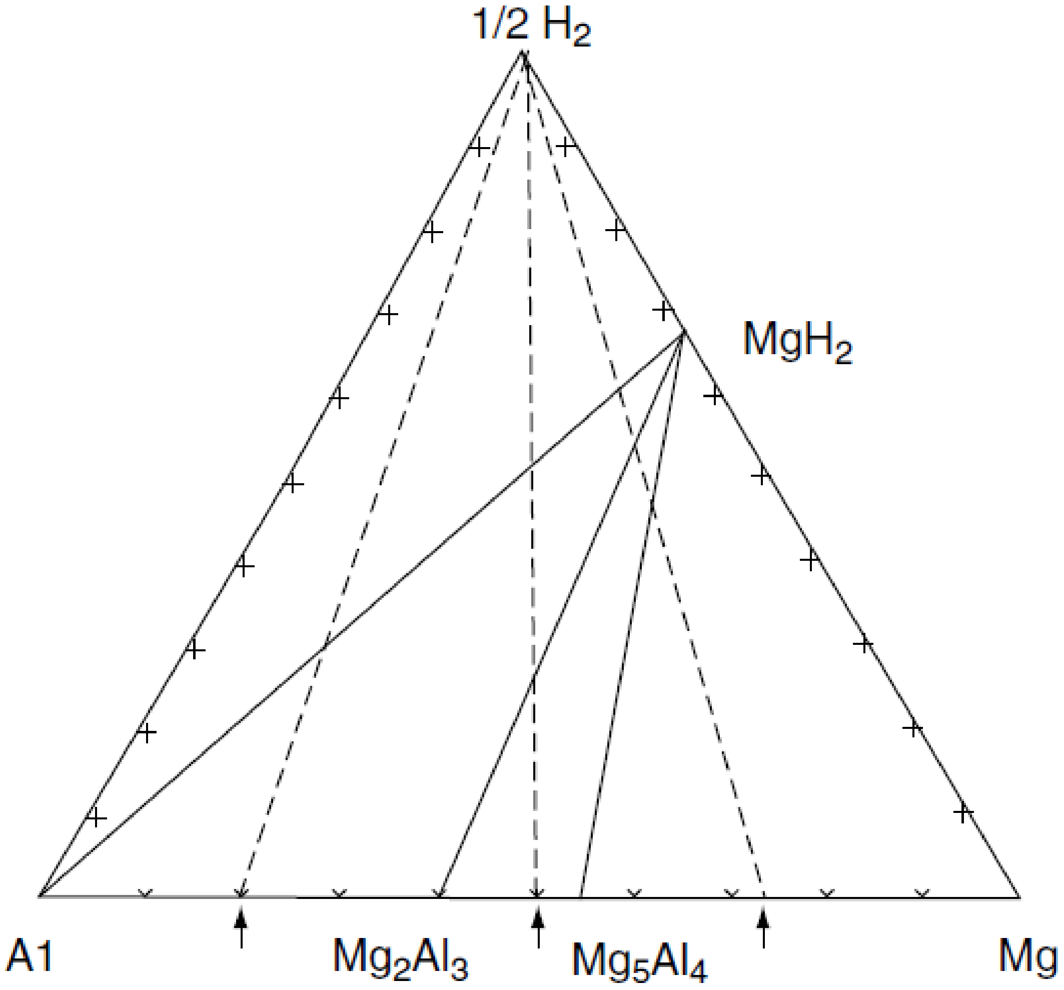

Fig. 4.21 Ternary phase stability diagram for the H–Mg–Al system at about 140°C, derived from the compositional variation of the potential as hydrogen was reacted with different initial binary alloy compositions using organic anion molten salt electrolyte

7. Ternary Examples: Lithium–Transition Metal Oxides

-LiCl-KCl eutectic molten salt as electrolyte at 400℃ (to develop large scale batteries for vehicle

-Li-cobalt oxide ternary system
CoO: Li↑ 1.807→1.603→0V
$LiCoO_2$: Li↑ only one voltage
jump from 1.636 to 0
(binary tie tine)

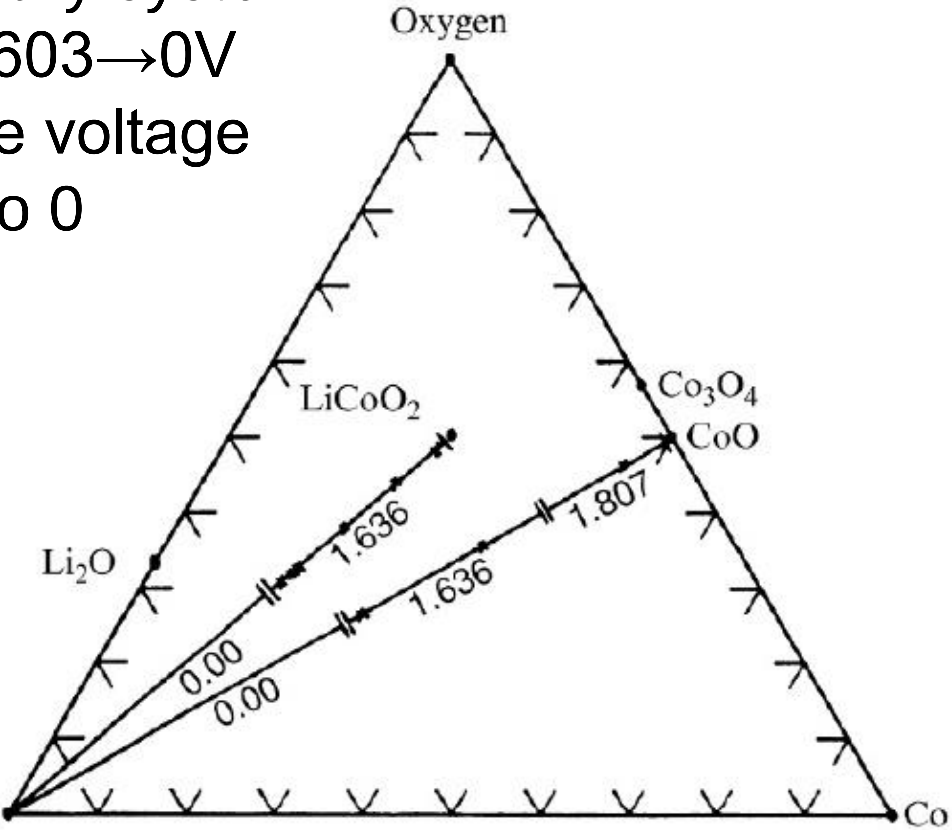

Fig. 4.22 Results of coulometric titration experiments on two compositions in the lithium–cobalt oxide system

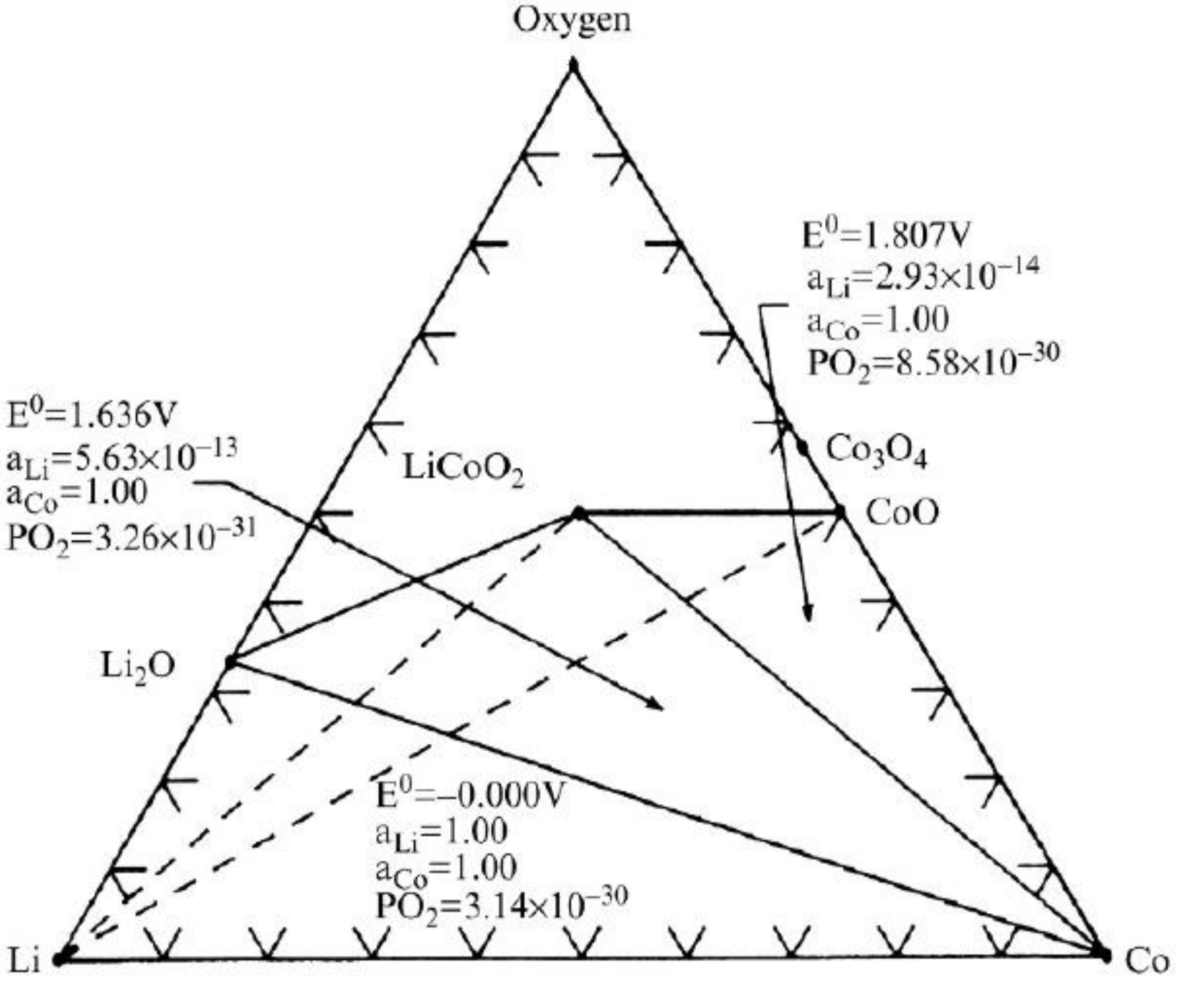

Fig. 4.23 Ternary phase stability diagram derived from the coulometric titration experiments shown in Fig. 4.22

Li-Fe-O system

Fe_3O_4: a small initial solid solution region → three jumps

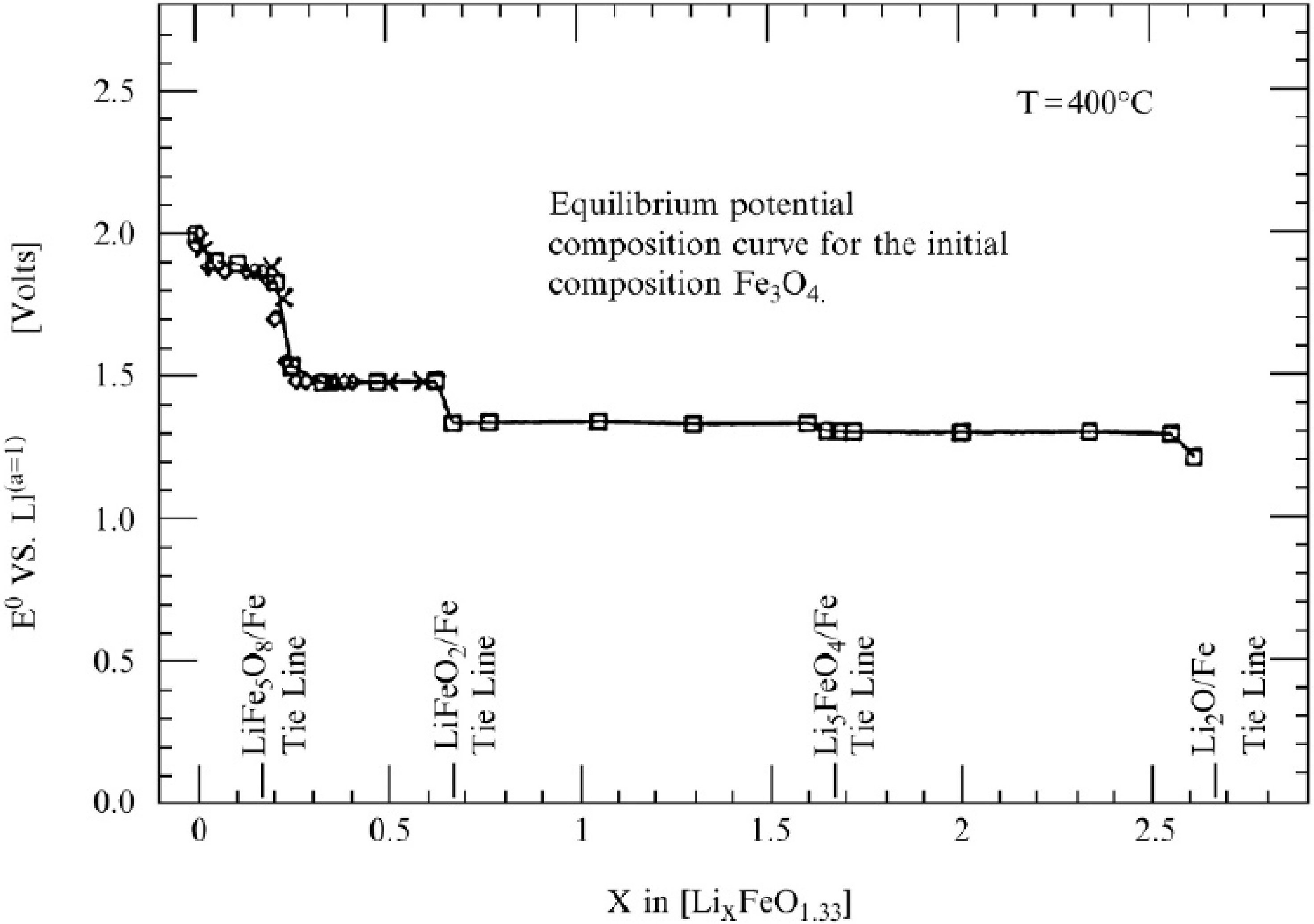

Fig. 4.24 Results of a coulometric titration experiment on a sample with an initial composition Fe_3O_4

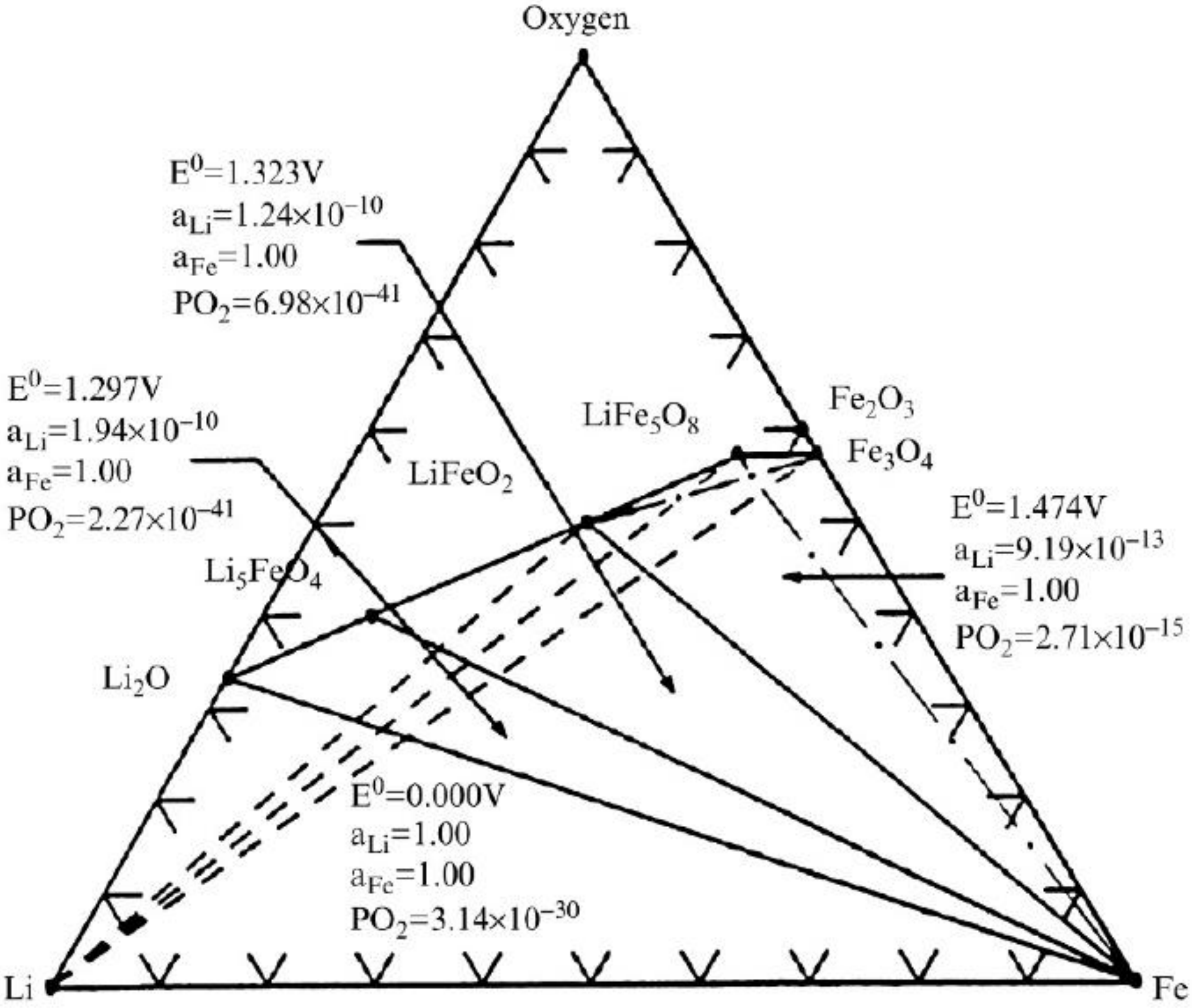

Fig. 4.25 Ternary phase stability diagram derived from coulometric titration measurements on materials in the Li–Fe–O ternary system

Li-Mn-O system

Initial compositions: MnO, Mn_3O_4, $LiMnO_2$, Li_2MnO_3

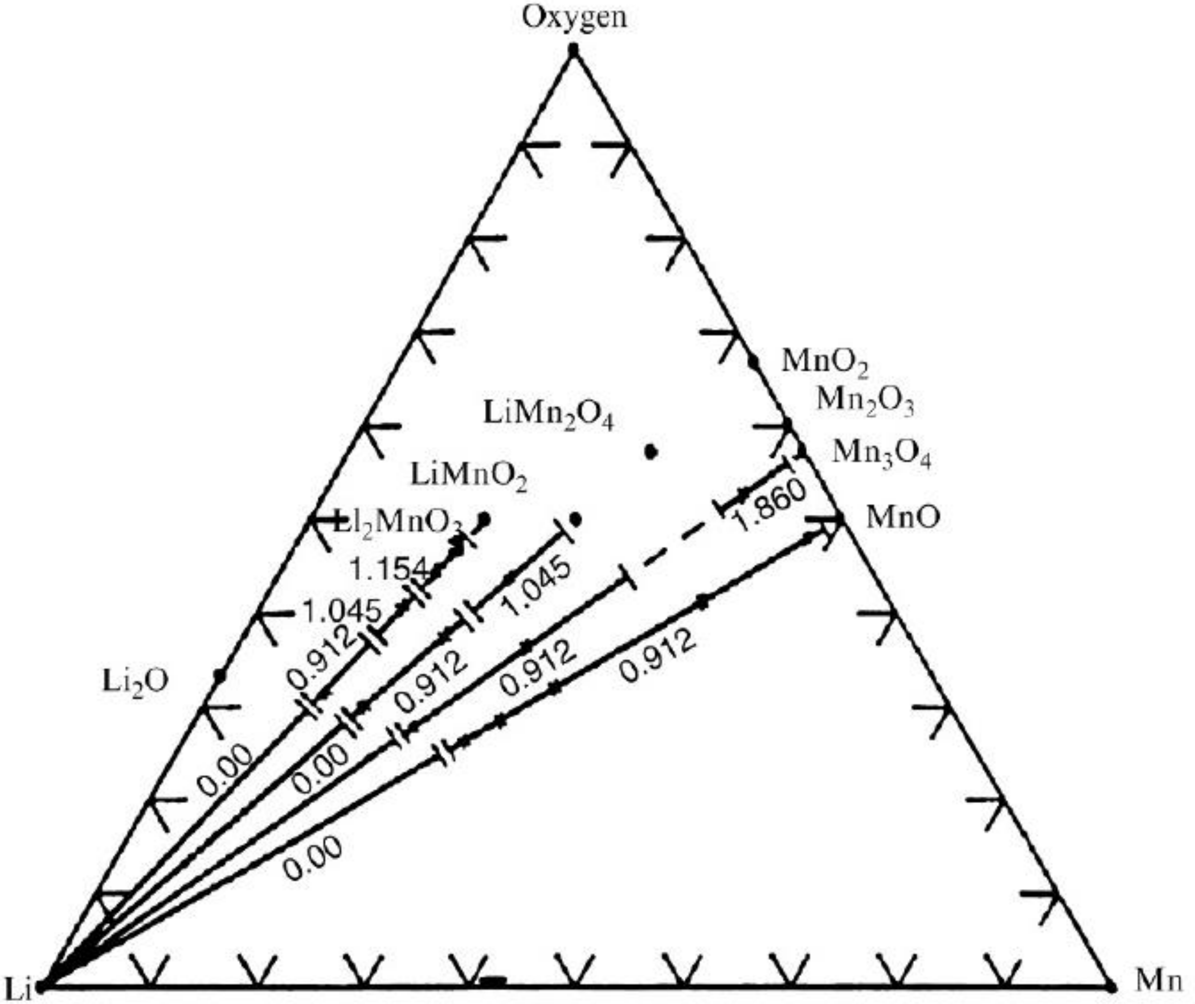

Fig. 4.26 Results of coulometric titration experiments on several phases in the Li–Mn–O ternary system

All the two phase tie lines do not go to the transition metal corner. Instead, three of them lead to the composition Li_2O

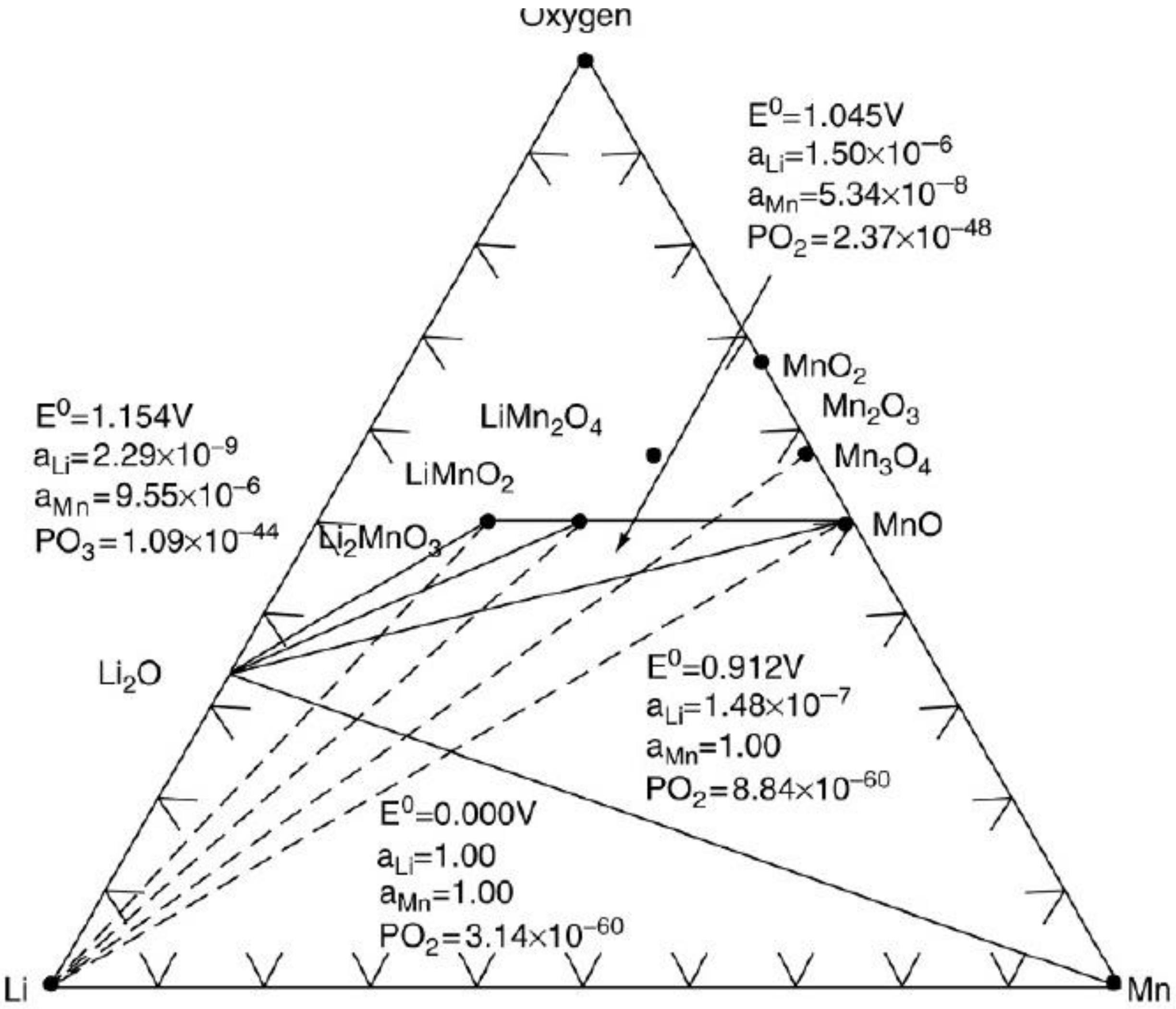

Fig. 4.27 Ternary phase stability diagram that resulted from the coulometric titration results shown in Fig. 4.26

8. Ternary Systems Composed of Two Binary Metal Alloys

All three components are metals: two binary lithium alloy Li-Cd, Li-Sn

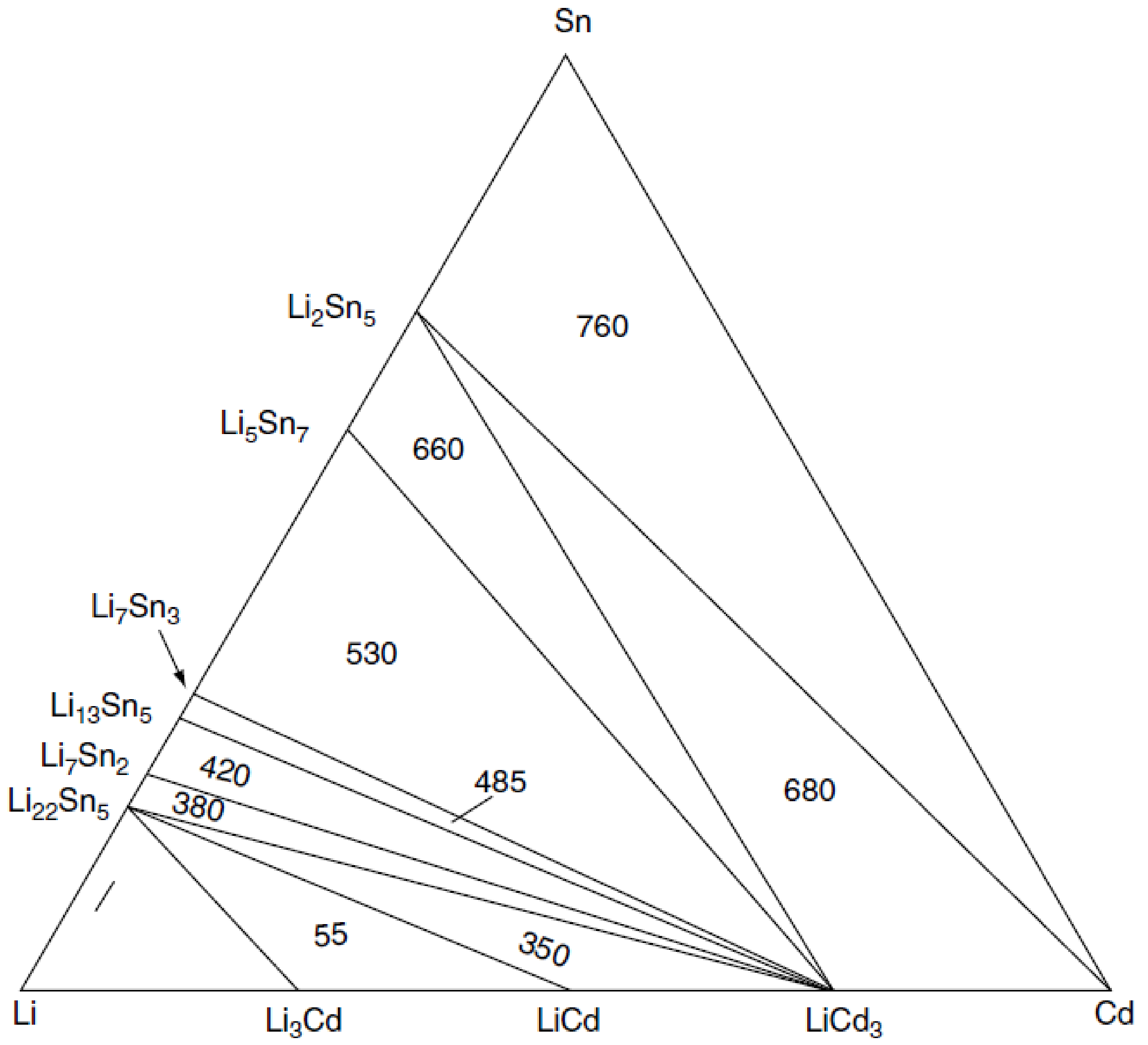

Fig. 4.28 Ternary phase stability diagram for the Li–Cd–Sn system. The numbers are the values of the voltage of all compositions in the various subtriangles relative to pure lithium